

# Synthesis, Structure, and Reactivity of Osmium Silyl and Silylene Complexes $\text{Cp}^*(\text{Me}_3\text{P})_2\text{OsSiR}_2\text{X}$ and $[\text{Cp}^*(\text{Me}_3\text{P})_2\text{OsSiR}_2][\text{B}(\text{C}_6\text{F}_5)_4]$ ( $\text{R} = \text{Me}, \text{}^i\text{Pr}$ ; $\text{X} = \text{Cl}, \text{OTf}$ )

Paul B. Glaser, Paulus W. Wanandi, and T. Don Tilley\*

Department of Chemistry and Center for New Directions in Organic Synthesis (CNDOS),  
University of California, Berkeley, Berkeley, California 94720-1460

Received September 19, 2003

Reaction of  $\text{Cp}^*(\text{Me}_3\text{P})_2\text{OsCH}_2\text{SiMe}_3$  (**1**,  $\text{Cp}^* = \text{C}_5\text{Me}_5$ ) with an excess of  ${}^i\text{Pr}_2\text{Si}(\text{H})\text{Cl}$  afforded  $\text{Cp}^*(\text{Me}_3\text{P})_2\text{OsSi}{}^i\text{Pr}_2\text{Cl}$  (**2**) in good yield, without the formation of Os(IV) products. Treatment of **2** with  $\text{Me}_3\text{SiOTf}$  ( $\text{OTf} = \text{triflate}, \text{OSO}_2\text{CF}_3$ ) afforded the corresponding triflatosilyl complex  $\text{Cp}^*(\text{Me}_3\text{P})_2\text{OsSi}{}^i\text{Pr}_2\text{OTf}$  (**3**), which appears to possess substantial silylene character, as determined by structural and spectroscopic measurements. The synthetic route to these complexes is analogous to that employed for the previously reported dimethylsilyl compounds  $\text{Cp}^*(\text{Me}_3\text{P})_2\text{OsSiMe}_2\text{X}$  ( $\text{X} = \text{Cl}$  (**4**),  $\text{OTf}$  (**5**)). Complexes **2–5** were converted to the corresponding base-free silylene complexes  $[\text{Cp}^*(\text{Me}_3\text{P})_2\text{Os}=\text{SiR}_2][\text{B}(\text{C}_6\text{F}_5)_4]$  ( $\text{R} = \text{Me}$  (**6**),  ${}^i\text{Pr}$  (**7**)) by anion metathesis with  $\text{Li}[\text{B}(\text{C}_6\text{F}_5)_4]\cdot 3\text{Et}_2\text{O}$ . Both **6** and **7** were characterized by multinuclear NMR spectroscopy and X-ray crystallography. The silylene complexes feature a trigonal planar environment for silicon, short Os–Si contacts (2.257(7) Å for **6**, 2.263(1) Å for **7**), and  ${}^{29}\text{Si}$  NMR resonances that are shifted to very low field (350 ppm for **6**; 363 ppm for **7**). The spectroscopic and structural differences between these silylene complexes and their precursors are discussed. While stable in fluorobenzene, **6** and **7** are rapidly oxidized by chlorocarbons via a radical pathway to form cationic Os(III) chlorosilyl species. Reactions of **7** with oxygen atom sources such as  $\text{N}_2\text{O}$  and 2-picoline *N*-oxide afforded the  $\text{N}_2$ -bridged diosmium complex  $[\text{Cp}^*(\text{Me}_3\text{P})_2\text{Os}-\text{NN}-\text{Os}(\text{PMe}_3)_2\text{Cp}^*][\text{B}(\text{C}_6\text{F}_5)_4]_2$  (**8**) and the cyclic siloxane  $(\text{OSi}{}^i\text{Pr}_2)_3$ . Reaction of **7** with elemental sulfur provided the turquoise,  $\text{S}_2$ -bridged diosmium complex  $[\text{Cp}^*(\text{Me}_3\text{P})_2\text{Os}-\text{S}-\text{S}-\text{Os}(\text{PMe}_3)_2\text{Cp}^*][\text{B}(\text{C}_6\text{F}_5)_4]_2$  (**9**) and unidentified silicon-containing products.

## Introduction

Metal-silylene complexes continue to be important synthetic targets in organometallic chemistry<sup>1</sup> due to their presumed participation in stoichiometric and catalytic processes involving silicon and because of their potential as catalysts for organic transformations. Notable among the processes believed to involve metal-silylene complexes are transfers of silylene fragments to unsaturated carbon–carbon bonds,<sup>2</sup> the Rochow

direct process for the synthesis of methylchlorosilanes,<sup>3</sup> and substituent redistribution reactions of organosilanes.<sup>4</sup> Synthetic methods employed in the preparation of silylene complexes include coordination of isolable<sup>5</sup> or photolytically generated<sup>6</sup> silylenes to an unsaturated metal center, abstraction of an anionic substituent from a silicon center,<sup>7</sup> or migration of a hydride from silicon to a coordinatively unsaturated metal center.<sup>8</sup>

The syntheses of a series of cationic, base-free and base-stabilized ruthenium silylene complexes  $[\text{Cp}^*$ -

(1) (a) Tilley, T. D. In *The Chemistry of Organosilicon Compounds*; Patai, S., Rappoport, Z., Eds.; 1989; Vol. 2, Chapter 24. (b) Tilley, T. D. In *The Silicon-Heteroatom Bond*; Patai, S., Rappoport, Z., Eds.; Wiley & Sons: New York, 1991; Chapter 10. (c) Zybail, C.; Handwerker, H.; Friedrich, H. *Adv. Organomet. Chem.* **1994**, *36*, 229. (d) Eisen, M. S. In *The Chemistry of Organosilicon Compounds*, Vol. 2; Rappoport, Z., Apeloig, Y., Eds.; Wiley & Sons: New York, 1998; Chapter 35. (e) Okazaki, M.; Tobita, H.; Ogino, H. *J. Chem. Soc., Dalton Trans.* **2003**, 493.

(2) (a) Seyferth, D.; Shannon, M. L.; Vick, S. C.; Lim, T. F. O. *Organometallics* **1985**, *4*, 57. (b) Cirakovic, J.; Driver, T. G.; Woerpel, K. A. *J. Am. Chem. Soc.* **2002**, *124*, 9370. (c) Palmer, W. S.; Woerpel, K. A. *Organometallics* **1997**, *16*, 4824. (d) Bodnar, P. M.; Palmer, W. S.; Ridgway, B. H.; Shaw, J. T.; Smitrovich, J. H.; Woerpel, K. A. *J. Org. Chem.* **1997**, *62*, 4737. (e) Palmer, W. S.; Woerpel, K. A. *Organometallics* **1997**, *16*, 1097. (f) Franz, A. K.; Woerpel, K. A. *J. Am. Chem. Soc.* **1999**, *121*, 949. (g) Palmer, W. S.; Woerpel, K. A. *Organometallics* **2001**, *20*, 3691. (h) Yamamoto, K.; Okinoshima, H.; Kumada, M. *J. Organomet. Chem.* **1970**, *23*, C7. (i) Yamamoto, K.; Okinoshima, H.; Kumada, M. *J. Organomet. Chem.* **1971**, *27*, C31. (j) Okinoshima, H.; Yamamoto, K.; Kumada, M. *J. Am. Chem. Soc.* **1972**, *94*, 9263. (k) Kumada, M.; Ishikawa, M.; Okinoshima, H.; Yamamoto, K. *Ann. NY Acad. Sci.* **1974**, *239*, 32. (l) Yamashita, H.; Tanaka, M. *Bull. Chem. Soc. Jpn.* **1995**, *68*, 403.

(3) (a) Lewis, K. M.; Rethwisch, D. G., Eds. *Catalyzed Direct Reactions of Silicon*; Elsevier: Amsterdam, 1993. (b) Walter, H.; Roewer, G.; Bohmhammel, K. *J. Chem. Soc., Faraday Trans.* **1996**, *92*, 4605. (c) Okamoto, M.; Onodera, S.; Okano, T.; Suzuki, E.; Ono, Y. *J. Organomet. Chem.* **1997**, *531*, 67. (d) Roewer, G.; Werkmeister, J.; Bohmhammel, K. In *Silicon for the Chemical Industry IV*; Geiranger: Norway, Jun 3–5, 1998; pp 239–252. (e) Acker, J.; Bohmhammel, K. *J. Phys. Chem. B* **2002**, *106*, 5105. (f) Pachaly, B.; Weis, J.; The Direct Process to Methylchlorosilanes: Reflections in Chemistry and Process Technology. In *Organosilicon Chemistry III: From Molecules to Materials, Munich Silicon Days*; Apr 3, 1996; Wiley & Sons: New York, 1998; p 478.

(4) (a) Curtis, M. D.; Epstein, P. S. *Adv. Organomet. Chem.* **1981**, *19*, 213. (b) Kumaada, M. *J. Organomet. Chem.* **1975**, *100*, 127.

(5) (a) Denk, M.; Hayashi, R. K.; West, R. *Chem. Commun.* **1994**, 33. (b) Gehrhus, B.; Hitchcock, P. B.; Lappert, M. F.; Maciejewski, H. *Organometallics* **1998**, *17*, 5599. (c) Petri, S. H. A.; Eikenberg, D.; Neumann, B.; Stammer, H. G.; Jutzli, P. *Organometallics* **1999**, *18*, 2615. (d) Cai, X. P.; Gehrhus, B.; Hitchcock, P. B.; Lappert, M. F.; Maciejewski, H. *Can. J. Chem.* **2000**, *78*, 1484. (e) Amoroso, D.; Haaf, M.; Yap, G. P. A.; West, R.; Fogg, D. E. *Organometallics* **2000**, *21*, 534.

(6) Feldman, J. D.; Mitchell, J. D.; Nölte, J. O.; Tilley, T. D. *J. Am. Chem. Soc.* **1998**, *120*, 11184.

(Me<sub>3</sub>P)<sub>2</sub>Ru=SiR<sub>2</sub>[BR'<sub>4</sub>] (Cp\* = C<sub>5</sub>Me<sub>5</sub>; R = Me, Ph, thiolate; R' = C<sub>6</sub>F<sub>5</sub>, Ph) from analogous triflatosilyl (triflate = OTf, OSO<sub>2</sub>CF<sub>3</sub>) derivatives served as a demonstration of the stability of donor-free metal-bound silylene complexes both with<sup>7c,e</sup> and without<sup>7f,h</sup> α-heteroatom stabilization, and established the utility of the anion metathesis methodology for the preparation of cationic silylene complexes. Such metathesis reactions replace a substituent on silicon, such as halide, triflate, or thiolate with an anionic group, such as a tetraarylborate, that does not coordinate to the resulting three-coordinate silicon center. Presumably, the electron-rich Cp\*(Me<sub>3</sub>P)<sub>2</sub>Ru<sup>+</sup> fragment stabilizes the formally unsaturated and highly electrophilic silylene ligands through the donation of electron density.

Osmium complexes are more electron-rich than analogous ruthenium species<sup>9</sup> and, therefore, should be more effective at stabilizing unsaturated ligands such as silylenes through metal-to-ligand back-bonding. Osmium has previously been shown to support a number of reactive, unsaturated fragments such as methylenes,<sup>10</sup> osmabenzene,<sup>11</sup> osmabenzynes,<sup>12</sup> vinylidenes,<sup>13</sup> thiocarbonyl,<sup>14</sup> and thioformyl.<sup>15</sup> Also, on the basis of observed periodic trends in bond strengths, bonds to osmium are expected to be stronger than those to ruthenium.<sup>9</sup> However, reports of complexes with osmium-silylene character are limited to the bimetallic complex (CO)<sub>4</sub>OsSi(S-tolyl-*p*)[RuCp\*(PMe<sub>3</sub>)<sub>2</sub>]<sup>7e</sup> and the silylene-THF adduct (THF)(TPP)OsSiEt<sub>2</sub>(THF)<sup>16</sup> (TPP

= tetratolylporphyrin). Given the successful syntheses of ruthenium silylene complexes such as Cp\*(R<sub>3</sub>P)<sub>2</sub>-RuSiMe<sub>2</sub><sup>+</sup> and the report in 1995 of a practical route to the previously elusive Cp\*(R<sub>3</sub>P)<sub>2</sub>Os<sup>+</sup> fragment,<sup>17</sup> osmium silylene complexes based on this ligand set were identified as viable and important synthetic targets.

In 1997, the synthesis of a series of osmium silyl species including Cp\*(Me<sub>3</sub>P)<sub>2</sub>OsSiMe<sub>2</sub>Cl (**4**) and Cp\*(Me<sub>3</sub>P)<sub>2</sub>OsSiMe<sub>2</sub>OTf (**5**) were reported.<sup>18</sup> Despite persistent difficulties in obtaining **4** in high yield, the isolation of these compounds demonstrated that the synthesis of a series of osmium complexes analogous to those successfully used as precursors to Cp\*(Me<sub>3</sub>P)<sub>2</sub>Ru=SiR<sub>2</sub><sup>+</sup> species was possible. Here, the synthesis and reactivity of a series of new osmium silyl and silylene complexes are reported, along with the first examples of structurally characterized osmium silylene complexes.

## Results and Discussion

**Synthesis of the Osmium Silyl Complexes Cp\*(Me<sub>3</sub>P)<sub>2</sub>OsSiR<sub>2</sub>Cl and Cp\*(Me<sub>3</sub>P)<sub>2</sub>OsSiR<sub>2</sub>OTf (R = Me, <sup>i</sup>Pr).** The previously reported synthesis of ruthenium silylene complexes [Cp\*(Me<sub>3</sub>P)<sub>2</sub>Ru=SiR<sub>2</sub>]<sup>+</sup> (R = alkyl, aryl, thiolate) required a series of ruthenium silyl derivatives that could be subjected to anion metathesis. Such silylene precursors were obtained from alkyl/silyl exchange reactions between Cp\*(Me<sub>3</sub>P)<sub>2</sub>RuCH<sub>2</sub>SiMe<sub>3</sub><sup>19</sup> and hydrosilanes such as R<sub>2</sub>Si(H)Cl (R = Me, Ph) and HSi(SR)<sub>3</sub> (R = C<sub>2</sub>H<sub>5</sub>, *p*-tolyl), to give the desired ruthenium silyl species and SiMe<sub>4</sub> as an elimination product.<sup>7b</sup> When carried out in a sealed vessel to prevent the loss of PMe<sub>3</sub> and concomitant formation of undesired Ru(IV) bis(silyl) species, these reactions proceed smoothly and in good yield.

As reported in 1997, reaction of Cp\*(Me<sub>3</sub>P)<sub>2</sub>OsCH<sub>2</sub>-SiMe<sub>3</sub> (**1**) with HSiMe<sub>2</sub>Cl affords a mixture of Cp\*(Me<sub>3</sub>P)<sub>2</sub>OsSiMe<sub>2</sub>Cl (**4**) and the undesired osmium bis(silyl) product Cp\*(Me<sub>3</sub>P)<sub>2</sub>Os(H)(SiMe<sub>2</sub>Cl)<sub>2</sub>.<sup>18</sup> These two products are not easily separated, and efforts to control the distribution of the products to favor **4** were largely unsuccessful. Attempts to introduce silylthiolato groups of the type -Si(SR)<sub>3</sub> at the osmium center led to metalated Os(IV) products. These difficulties, largely absent in the analogous ruthenium system, can be attributed to the proclivities of osmium to attain a formal oxidation state of +4 and engage in orthometalation pathways. With the hope that a sterically demanding silyl group might disfavor the formation of bis(silyl) species, the synthesis of an osmium diisopropylsilyl complex was targeted.

Reaction of **1** in neat <sup>i</sup>Pr<sub>2</sub>Si(H)Cl at elevated temperature led to formation of the osmium silyl complex Cp\*(Me<sub>3</sub>P)<sub>2</sub>OsSi<sup>i</sup>Pr<sub>2</sub>Cl (**2**) in good yield. In marked contrast to the problematic reaction of **1** with Me<sub>2</sub>Si(H)Cl, formation of the bis(silyl) Os(IV) compound Cp\*(Me<sub>3</sub>P)Os(H)(Si<sup>i</sup>Pr<sub>2</sub>Cl)<sub>2</sub> was not observed. This result may be attributed to the increased steric demands of the diisopropylsilyl group, which disfavor a second Si-H oxidative addition (Scheme 1).

(17) Gross, C. L.; Wilson, S. R.; Girolami, G. S. *J. Am. Chem. Soc.* **1994**, *116*, 10294.

(18) Wanandi, P. W.; Tilley, T. D. *Organometallics* **1997**, *16*, 4299.

(19) Tilley, T. D.; Grubbs, R. H.; Bercaw, J. E. *Organometallics* **1984**, *3*, 274.

(7) (a) Straus, D. A.; Tilley, T. D.; Reingold, A. L.; Geib, S. J. *J. Am. Chem. Soc.* **1987**, *109*, 5872. (b) Straus, D. A.; Zhang, C.; Quimbata, G. E.; Grumbine, S. D.; Heyn, R. H.; Tilley, T. D.; Rheingold, A. L.; Geib, S. J. *J. Am. Chem. Soc.* **1990**, *112*, 2673. (c) Straus, D. A.; Grumbine, S. D.; Tilley, T. D. *J. Am. Chem. Soc.* **1990**, *112*, 7801. (d) Grumbine, S. D.; Chadha, R. K.; Tilley, T. D. *J. Am. Chem. Soc.* **1992**, *114*, 1518. (e) Grumbine, S. D.; Tilley, T. D.; Rheingold, A. L. *J. Am. Chem. Soc.* **1993**, *115*, 358. (f) Grumbine, S. K.; Tilley, T. D.; Arnold, F. P.; Rheingold, A. L. *J. Am. Chem. Soc.* **1994**, *116*, 5495. (g) Grumbine, S. K.; Straus, D.; Tilley, T. D. *Polyhedron* **1995**, *14*, 127. (h) Grumbine, S. K.; Mitchell, G. P.; Straus, D. A.; Tilley, T. D.; Rheingold, A. L. *Organometallics* **1998**, *17*, 5607. (i) Grumbine, S. D.; Tilley, T. D.; Arnold, F. P.; Rheingold, A. L. *J. Am. Chem. Soc.* **1993**, *115*, 7884. (j) Klei, S. R.; Tilley, T. D.; Bergman, R. G. *Organometallics* **2002**, *21*, 4648.

(8) (a) Mitchell, G. P.; Tilley, T. D. *Angew. Chem., Int. Ed.* **1998**, *37*, 2524. (b) Feldman, J. D.; Peters, J. C.; Tilley, T. D. *Organometallics* **2002**, *21*, 4065–4075. (c) Peters, J. C.; Feldman, J. D.; Tilley, T. D. *J. Am. Chem. Soc.* **1999**, *121*, 9871–9872. (d) Mork, B. V.; Tilley, T. D. *J. Am. Chem. Soc.* **2001**, *123*, 9702–9703. (e) Klei, S. R.; Tilley, T. D.; Bergman, R. G. *J. Am. Chem. Soc.* **2000**, *122*, 1816–1817.

(9) (a) Cotton, A. F.; Wilkinson, G. *Advanced Inorganic Chemistry*; Wiley-Interscience: New York, 1980. (b) Crabtree, R. H. *The Organometallic Chemistry of the Transition Metals*; Wiley: New York, 2001. (c) Sánchez-Delgado, R. A.; Rosales, M.; Esteruelas, M. A.; Oro, L. A. *J. Mol. Catal. A* **1995**, *96*, 231.

(10) (a) Hill, A. F.; Roper, W. R.; Waters, J. M.; Wright, A. H. *J. Am. Chem. Soc.* **1983**, *105*, 5939. (b) Brumaghim, J. L.; Girolami, G. S. *Chem. Commun.* **1999**, 953. (c) Roder, K.; Werner, H. *J. Organomet. Chem.* **1989**, *367*, 321. (d) Huang, D.; Spivak, G. J.; Caulton, K. G. *New J. Chem.* **1998**, *22*, 1023. (e) Werner, H.; Stuer, W.; Wolf, J.; Laubender, M.; Weberndorfer, B.; Herbst-Irmer, R.; Lehmann, C. *Eur. J. Inorg. Chem.* **1999**, *11*, 1889.

(11) (a) Blecke, J. R. *Chem. Rev.* **2001**, *101*, 1205. (b) Elliott, G. P.; Roper, W. R.; Waters, J. M. *Chem. Commun.* **1982**, 811.

(12) (a) Bin Wen, T.; Zhou, Z. Y.; Jia, G. C. *Angew. Chem., Int. Ed.* **2001**, *40*, 1951. (b) Roper, W. R. *Angew. Chem., Int. Ed.* **2001**, *40*, 2440.

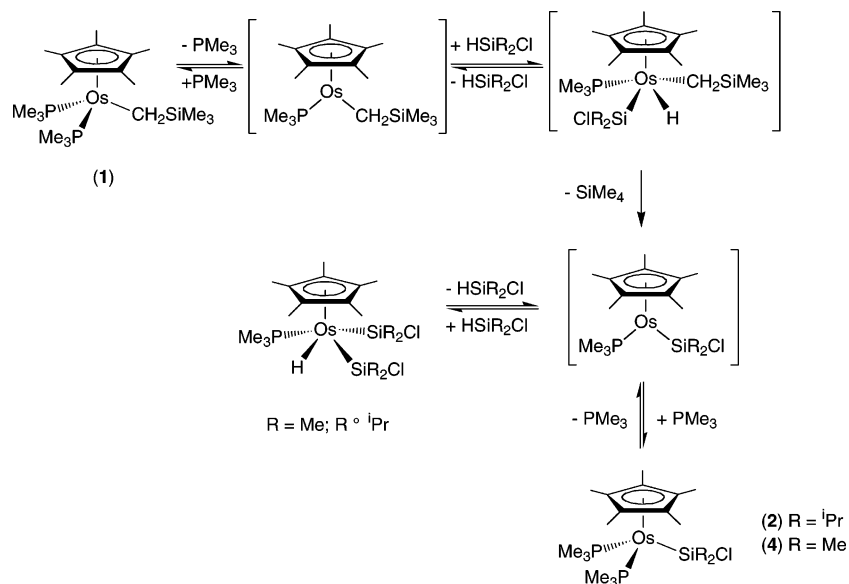
(13) (a) Baya, M.; Crochet, P.; Esteruelas, M. A.; Lopez, A. M.; Modrego, J. *Organometallics* **2001**, *20*, 4291. (b) Puerta, M. C.; Valerga, P. *Coord. Chem. Rev.* **1999**, *195*, 977. (c) Bin Wen, T.; Yang, S. Y.; Zhou, Z. Y.; Lin, Z. Y.; Lau, C. P.; Jia, G. C. *Organometallics* **2000**, *19*, 3757.

(14) (a) Collins, T. J.; Roper, W. R.; Town, K. G. *J. Organomet. Chem.* **1976**, *121*, C41–C44. (b) Clark, G. R.; Marsden, K.; Roper, W. R.; Wright, L. J. *J. Am. Chem. Soc.* **1980**, *102*, 1206–1207.

(15) (a) Collins, T. J.; Roper, W. R. *Chem. Commun.* **1976**, 1044. (b) Collins, T. J.; Roper, W. R. *J. Organomet. Chem.* **1978**, *159*, 73.

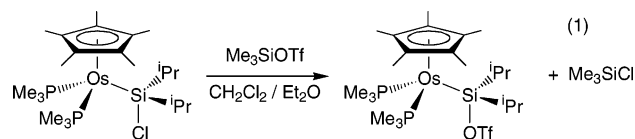
(16) Woo, L. K.; Smith, D. A.; Young, V. G. *Organometallics* **1991**, *10*, 3977.

## Scheme 1



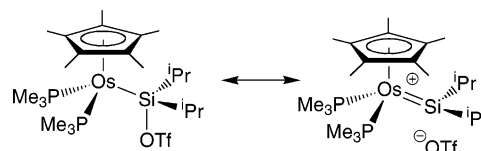
Crystals of **2** suitable for X-ray crystallography were grown from a concentrated pentane solution at  $-30\text{ }^{\circ}\text{C}$ . The solid state structure of **2** (Figure 1) features a silicon center that is clearly tetrahedral and an Os–Si bond length of  $2.404(3)\text{ \AA}$ . The Si–Cl bond of  $2.209(4)\text{ \AA}$  is unusually long,<sup>20</sup> presumably as a result of substantial donation by the electron-rich metal center into the Si–Cl  $\sigma^*$  orbital.

Using an established metathesis protocol employing  $\text{Me}_3\text{SiOTf}$ ,<sup>7b,18</sup> **2** was cleanly converted to  $\text{Cp}^*(\text{Me}_3\text{P})_2\text{-OsSi}^i\text{Pr}_2\text{OTf}$  (**3**) (eq 1). This complex crystallizes readily



from  $\text{CH}_2\text{Cl}_2/\text{Et}_2\text{O}$  solution as large hexagonal plates. The molecular structure of **3** is shown in Figure 2. At  $2.369(2)\text{ \AA}$ , the Os–Si bond in **3** is  $0.035\text{ \AA}$  shorter than the corresponding bond in **2**. In addition, the silicon–oxygen contact of  $1.910(7)\text{ \AA}$  for **3** is unusually long,<sup>21</sup> suggesting that the structure of **3** has a significant

## Scheme 2



contribution from a “no-bond” silylene resonance form (Scheme 2). As previously reported,<sup>18</sup> the Si–O bond in **5** is  $1.866(5)\text{ \AA}$ . The longer Si–O bond length in **3** is consistent with the increased steric demands of the two isopropyl groups relative to those of the methyl groups of **5**.

A useful structural parameter for describing the amount of silylene character at a metal-bound silicon atom is the sum of the bond angles about Si, excluding the anionic substituent.<sup>7g</sup> This sum approaches the value of  $360^{\circ}$  associated with a trigonal planar coordination environment as the degree of silylene character increases. Whereas the sum of the C–Si–C and two Os–Si–C bond angles in **2** is approximately  $340.3^{\circ}$ , the sum of the three corresponding angles in **3** is  $349.5^{\circ}$ , indicating greater silylene character in **3**.

The NMR spectroscopy of **3** provides key information regarding the nature of the silicon center in **3**. In  $\text{C}_6\text{D}_6$ ,

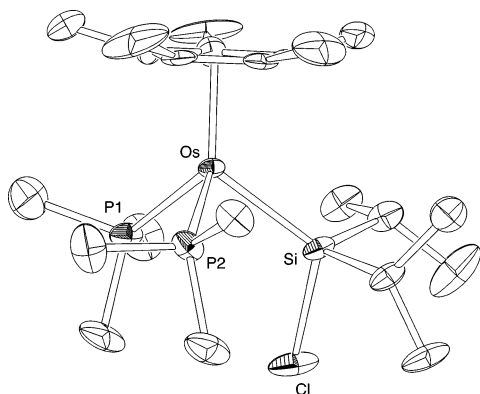


**Figure 1.** ORTEP diagram of **2** with thermal ellipsoids shown at the 50% probability level. Hydrogen atoms are omitted for clarity. Selected bond lengths ( $\text{\AA}$ ): Os–Si  $2.404(3)$ , Si–Cl  $2.209(4)$ . Sum of bond angles about silicon =  $340.3^{\circ}$ .

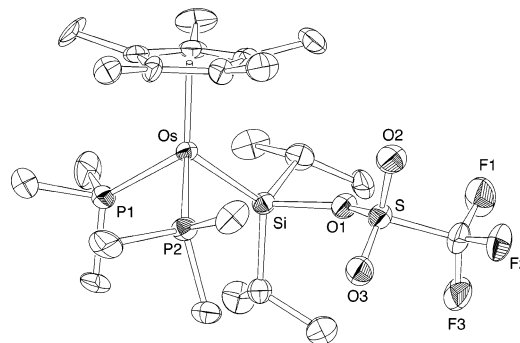
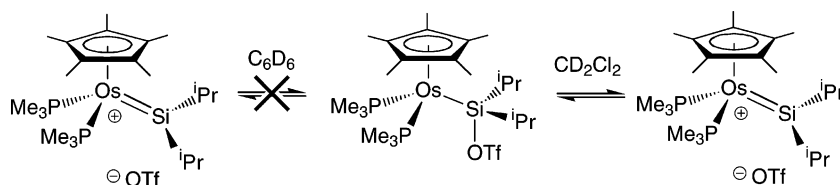


**Figure 2.** ORTEP diagram of **3** with thermal ellipsoids shown at the 50% probability level. Hydrogen atoms have been omitted for clarity. Selected bond lengths ( $\text{\AA}$ ): Os–Si  $2.368(2)$ , Si–O(1)  $1.907(7)$ . Sum of bond angles about silicon =  $349.5^{\circ}$ .

Scheme 3



**3** exhibits a  $^{29}\text{Si}$  chemical shift of 100 ppm, a value most consistent with tetravalent (vs  $\text{sp}^2$ ) silicon in a metal-silyl complex.<sup>22</sup> Interestingly, in the more polar solvent  $\text{CD}_2\text{Cl}_2$ , the  $^{29}\text{Si}$  resonance of **3** is shifted downfield to 223 ppm. This value is downfield of those reported for donor-stabilized silylene complexes of ruthenium and iron (e.g.,  $\delta(^{29}\text{Si})$  for  $[\text{Cp}^*(\text{Me}_3\text{P})_2\text{RuSiPh}_2(\text{NCMe})][\text{BPh}_4] = 95.75 \text{ ppm}^{7b}$ ) and closer to the values observed for the silicon centers in donor-free silylenes (e.g.,  $\delta(^{29}\text{Si})$  for  $[\text{Cp}^*(\text{Me}_3\text{P})_2\text{RuSiMe}_2][\text{B}(\text{C}_6\text{F}_5)_4] = 311.4 \text{ ppm}^{7c}$ ). Furthermore, the  $^1\text{H}$  NMR spectra of **3** in  $\text{C}_6\text{D}_6$  and  $\text{CD}_2\text{Cl}_2$  differ significantly. In  $\text{C}_6\text{D}_6$  at 25 °C, the methyl groups of each isopropyl group are diastereotopic and appear as two distinct doublets in  $^1\text{H}$  NMR spectra. Apparently, the more polar solvent  $\text{CD}_2\text{Cl}_2$  promotes triflate dissociation from the silicon center of **3**. Consequently, the isopropyl methyl groups in **3** appear as a single resonance in  $\text{CD}_2\text{Cl}_2$ , consistent with both fast inversion at the silicon center and unhindered rotation about the Os–Si bond on the NMR time scale. The  $^1\text{H}$  NMR spectrum of **3** in  $\text{CD}_2\text{Cl}_2$  remains essentially invariant over the temperature range  $-50$  to 25 °C. Similar spectroscopic properties are observed for other triflatosilyl complexes in which triflate is labile in solution.<sup>7h,23</sup>

Solely on the basis of NMR spectroscopic evidence, it is not possible to rule out the possibility that the triflate counterion is completely dissociated from the silicon center in  $\text{CD}_2\text{Cl}_2$ , that is, that the equilibrium depicted in Scheme 3 lies completely to the right. However, the  $^{29}\text{Si}$  chemical shift of 223 is consistent with some degree of interaction between the silicon center and the triflate counterion.<sup>24</sup> By analogy to ruthenium silylene complexes, a base-free silylene complex of osmium lacking  $\alpha$ -heteroatom stabilization would be expected to exhibit a  $^{29}\text{Si}$  chemical shift significantly downfield of 223

ppm.<sup>7f,h</sup> Furthermore,  $\text{CD}_2\text{Cl}_2$  solutions of **3** are stable for months without apparent decomposition. This stability contrasts with the rapid reaction observed between the corresponding silylene complex and chlorocarbons (vide infra). Considering all the spectroscopic data, **3** can be viewed as possessing a significant degree of silylene character in the solid state and in  $\text{C}_6\text{D}_6$  solution, and  $\text{CD}_2\text{Cl}_2$  promotes dissociation of the triflate anion to transiently afford a silylene complex formulated as  $[\text{Cp}^*(\text{Me}_3\text{P})_2\text{Os}=\text{Si}^i\text{Pr}_2][\text{OTf}]$ .

Interestingly, solutions of **3** exhibit different colors depending on the nature of the solvent. For example,  $\text{C}_6\text{D}_6$  solutions of **3** are very pale yellow, while  $\text{CD}_2\text{Cl}_2$  solutions are an intense lemon yellow color, a color associated in this system with the presence of a metal-silylene complex.

**Synthesis and Characterization of Osmium Silylene Complexes  $[\text{Cp}^*(\text{Me}_3\text{P})_2\text{Os}=\text{SiR}_2][\text{B}(\text{C}_6\text{F}_5)_4]$  ( $\text{R} = \text{Me}$ ,  $^i\text{Pr}$ ).** Initial attempts to generate an osmium silylene complex by treatment of the triflatosilyl complex  $\text{Cp}^*(\text{Me}_3\text{P})_2\text{OsSiMe}_2\text{OTf}$  with an equivalent of the anion-metathesis reagent  $\text{Li}[\text{B}(\text{C}_6\text{F}_5)_4]\cdot 3\text{Et}_2\text{O}$  in  $\text{CH}_2\text{Cl}_2$  were unsuccessful and led to a deeply colored mixture of paramagnetic (by NMR spectroscopy) and diamagnetic products. Since analogous ruthenium silylene species were prepared in and recrystallized from dichloromethane solution,<sup>7f,h</sup> the inability to synthesize an isolable osmium silylene complex under similar conditions was surprising. It was postulated that the desired silylene complex was generated in the anion metathesis reaction, but it quickly decomposed via a pathway involving the chlorinated solvent. To circumvent this synthetic difficulty, a solvent less reactive than dichloromethane but still polar enough to dissolve the product ion pair was chosen for the synthesis of an osmium silylene complex.

Reaction of the triflatosilyl complex **3** or **5** with  $\text{Li}[\text{B}(\text{C}_6\text{F}_5)_4]\cdot 3\text{Et}_2\text{O}$  in fluorobenzene solution led to rapid formation of the bright yellow silylene complexes  $[\text{Cp}^*(\text{Me}_3\text{P})_2\text{Os}=\text{SiR}_2][\text{B}(\text{C}_6\text{F}_5)_4]$  ( $\text{R} = \text{Me}$  (**6**),  $^i\text{Pr}$  (**7**)) with concomitant elimination of  $\text{LiOTf}$ . The paramagnetic species observed in the reaction of **3** with  $\text{Li}[\text{B}(\text{C}_6\text{F}_5)_4]\cdot 3\text{Et}_2\text{O}$  in  $\text{CD}_2\text{Cl}_2$  were not detected by NMR, and rapid color changes did not occur. The NMR spectroscopic properties of **7** in fluorobenzene are very similar to those of **3** in  $\text{CD}_2\text{Cl}_2$  with one notable exception: the  $^{29}\text{Si}$  resonance for **7** appears at 363 ppm, which is consistent with a three-coordinate silicon center in the complex.

Slow diffusion of hexanes into a fluorobenzene solution containing **7** and residual diethyl ether from the  $\text{Li}[\text{B}(\text{C}_6\text{F}_5)_4]\cdot 3\text{Et}_2\text{O}$  reagent afforded large crystals suitable for X-ray crystallography (Figure 3). Within error, the sum of the bond angles about the silicon center is  $360^\circ$ , indicating  $\text{sp}^2$  hybridization and the absence of any inter- or intramolecular interactions that might pyramidalize the silicon center in the solid state. The Os–

(20) A search of the Cambridge Crystallographic Structure Database revealed that the terminal Si–Cl bond in **2** is the longest such bond in crystallographically characterized transition metal complexes. The median bond length for all crystallographically characterized Si–Cl bonds is 2.063 Å.

(21) (a) A search of the Cambridge Crystallographic Structure Database revealed that the Si–O bond in **3** is the among the longest crystallographically characterized bonds between four-coordinate silicon and oxygen. The silanimine-benzophenone adduct  $(\text{tBu}_3\text{Si})\text{N}=\text{Si}(\text{tBu})_2\text{OCPh}_2$ <sup>21b</sup> is the only compound with a longer Si–O bond (1.926 Å). The median bond length for all crystallographically characterized bonds between four-coordinate silicon and oxygen is 1.635 Å. (b) Wiberg, N.; Schurz, K.; Müller, G.; Riede, J. *Angew. Chem., Int. Ed. Engl.* **1988**, *27*, 935.

(22) Corey, J. Y.; Braddock-Wilking, J. *Chem. Rev.* **1999**, *99*, 175–292.

(23) Lee, K. E.; Gladysz, J. A. *Polyhedron* **1988**, *7*, 2209.

(24) The  $^{29}\text{Si}$  chemical shift of three-coordinate silicium ions has been shown by computational methods to be sensitive to nucleophiles as weak as argon. By analogy, a similar sensitivity to very weakly nucleophilic species such as triflate is expected for silylene complexes. (a) Maerker, C.; Kapp, J.; Schleyer, P. v. R. In *Organosilicon Chemistry: From Molecules to Materials*, Vol. II; Auner, N., Weis, J., Eds.; VCH: Weinheim, 1995; p 329. (b) Maerker, C.; Schleyer, P. v. R. In *The Chemistry of Organosilicon Compounds*, Vol. 2; Rappoport, Z., Apeloig, Y., Eds.; Wiley & Sons: New York, 1998; Chapter 10.

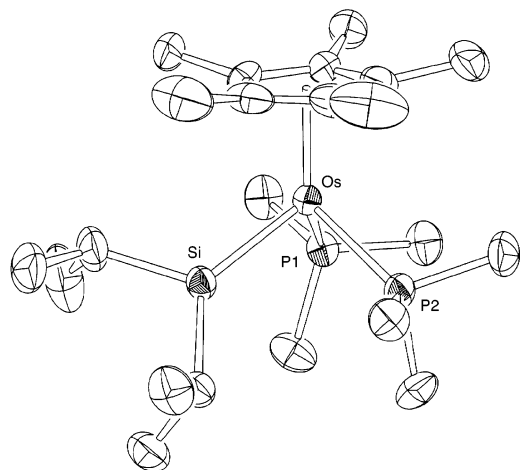


**Figure 3.** ORTEP diagram of **7** with thermal ellipsoids shown at the 50% probability level. Hydrogen atoms, the  $B(C_6F_5)_4$  counterion, and *n*-hexane of crystallization have been omitted for clarity. Os–Si bond length = 2.263(1) Å. Sum of angles about Si = 359.9°.

Si bond length in **7** (2.263(1) Å) is shorter than all other crystallographically characterized Os–Si bonds except for the 2.254(2) Å bond in  $Os(SiF_3)Cl(CO)(PPh_3)_2$ .<sup>25</sup>

The <sup>29</sup>Si chemical shift for **6** of 350 ppm is also consistent with a base-free silylene complex. Crystals suitable for X-ray crystallography were grown in a manner analogous to that used for **7**. Unfortunately, refinement of accurate metric parameters for **6** was confounded by a pernicious rotational disorder involving the Cp\* ring. Two different data sets were collected, solved, and refined, with similar results. A disorder model including two Cp\* rings at partial occupancy allowed refinement to a reasonable *R* value. Despite the problems in the refinement of this structure, a short Os–Si contact of 2.247(7) Å and a planar coordination environment for the silicon atom are clearly evident (Figure 4).<sup>26</sup> The prolate thermal ellipsoids of the silicon-bound carbon atoms have major axes roughly parallel to each other and almost orthogonal to the Os–Si vector, an arrangement most consistent with significant librational motion about this bond in the solid state.

The structural and spectroscopic data for the previously reported osmium silylene complexes differ markedly from those observed for **6** and **7**. For example, (THF)(TPP)OsSiEt<sub>2</sub>(THF) exhibits a <sup>29</sup>Si chemical shift of 24.5 ppm and a four-coordinate silicon center.<sup>16</sup> The bimetallic silylene complex (CO)<sub>4</sub>OsSi(S-tolyl-*p*)[RuCp\*(PMe<sub>3</sub>)<sub>2</sub>],<sup>7e</sup> while having a planar, three-coordinate silicon center, exhibits a <sup>29</sup>Si NMR shift of 19.43 ppm and an Os–Si bond length of 2.419(2) Å, which is significantly longer than the corresponding bond in **2**. Therefore, these previously reported osmium–silicon compounds appear to have far less silylene character than that possessed by **6** and **7**.

In contrast to the analogous ruthenium silylene complexes, **6** and **7** were found to be accessible from the

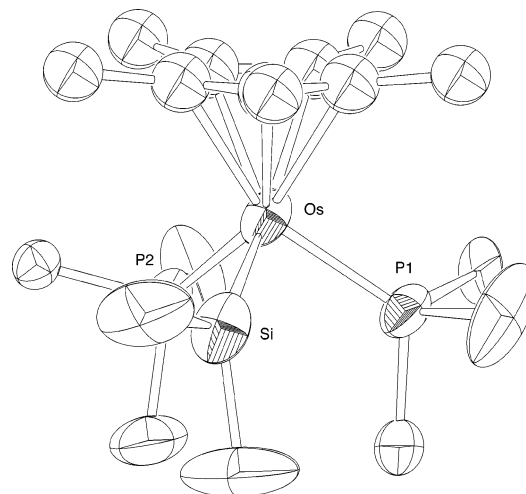


**Figure 4.** ORTEP diagram of **6** with thermal ellipsoids shown at the 50% probability level. Hydrogen atoms and the  $B(C_6F_5)_4$  counterion are omitted for clarity. The major contributor to the Cp\* disorder model is shown. Os–Si = 2.257(7) Å. Sum of angles about Si = 359.5°.

**Table 1.** Selected Structural and <sup>29</sup>Si NMR Data for Six Cp\*(Me<sub>3</sub>P)<sub>2</sub>OsSiR<sub>2</sub>X Complexes

	X		
	Cl	OTf	$B(C_6F_5)_4$
R = <i>i</i> Pr	<b>2</b>	<b>3</b>	<b>7</b>
Os–Si (Å)	2.404(3)	2.368(2)	2.263(1)
Σ∠(Si) <sup>d</sup>	340.3°	349.5°	359.9°
δ <sup>29</sup> Si (ppm)	61 <sup>a</sup>	100 <sup>b</sup> , 223 <sup>a</sup>	365 <sup>c</sup>
R = Me	<b>4</b> <sup>18</sup>	<b>5</b> <sup>18</sup>	<b>6</b>
Os–Si (Å)	2.334(2)	2.334(2)	2.257(7)
Σ∠(Si)	343.5°	343.5°	359.5°
δ <sup>29</sup> Si (ppm)	46.76 <sup>b</sup>	83.43 <sup>b</sup>	350 <sup>c</sup>

<sup>a</sup> Solvent = CD<sub>2</sub>Cl<sub>2</sub>. <sup>b</sup> Solvent = C<sub>6</sub>D<sub>6</sub>. <sup>c</sup> Solvent = 90% C<sub>6</sub>H<sub>5</sub>F + 10% C<sub>6</sub>D<sub>6</sub>. <sup>d</sup> Σ∠(Si) = sum of bond angles around silicon, excluding those involving Si–X.

corresponding silyl chloride complexes. In fluorobenzene, treatment of **2** or **4** with Li[B(C<sub>6</sub>F<sub>5</sub>)<sub>4</sub>]<sub>3</sub>Et<sub>2</sub>O afforded the silylene complexes with concomitant elimination of LiCl. However, despite the extra synthetic step required to prepare them, the corresponding triflate complexes are more convenient precursors to silylene complexes, as they exhibit greater crystallinity and are therefore more readily purified and isolated.

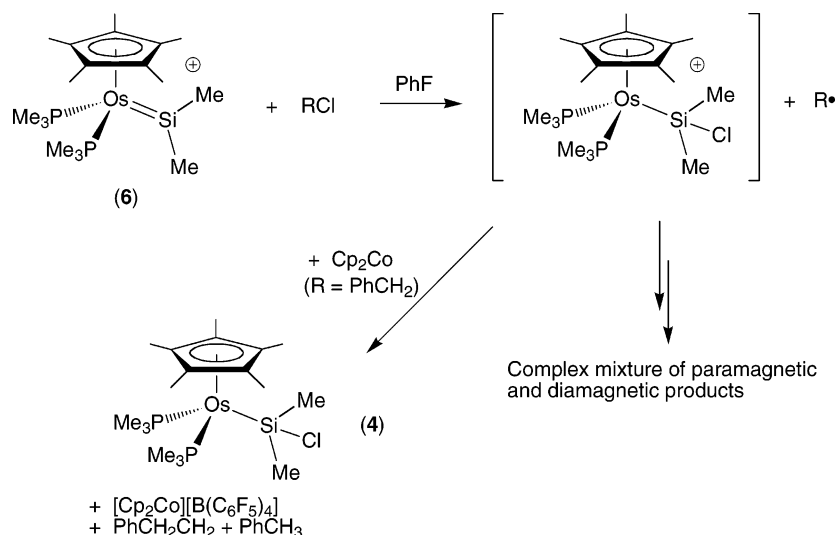
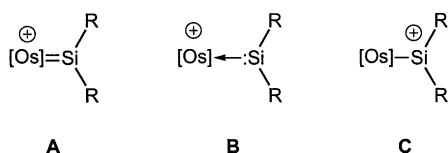
As a series, **2**, **3**, and **7** represent three points on the continuum between osmium silyl and osmium silylene complexes. As the anionic substituent associated with silicon is changed from chloride to triflate to tetrakis(pentafluorophenyl)borate, the Os–Si bond shortens and the coordination environment of the silicon center becomes more planar, consistent with an increasing degree of sp<sup>2</sup> hybridization at Si and increased double-bond character in the metal–silicon interaction. The trend in <sup>29</sup>Si chemical shifts is also consistent with increasing silylene character (Table 1).

Although short Os–Si bonds observed in **6** and **7** suggest the existence of a double bond, there is no indication of hindered rotation about the Os–Si bond in either of these complexes in solution, as observed by NMR spectroscopy at temperatures as low as –40 °C. Consequently, other resonance forms with Os–Si single bonds (e.g., **B** and **C**) may contribute significantly to the structure of the osmium silylene complexes (Chart 1).

(25) Hübler, K.; Hunt, P. A.; Maddock, S. M.; Rickard, C. E. F.; Roper, W. R.; Salter, D. M.; Schwerdtfeger, P. *Organometallics* **1997**, *16*, 5076.

(26) The disorder in the Cp\* ring and the magnitude of the associated uncertainty preclude a meaningful comparison of the length of the Os–Si bond in **6** to the analogous bond in **7**. It is, however, significantly shorter than the Os–Si bond of 2.334(2) Å in **5**.

Scheme 4

Chart 1<sup>a</sup>

<sup>a</sup>  $[\text{Os}] = \text{Cp}^*(\text{PMe}_3)_2\text{Os}$ .

**Reactions of Osmium Silylene Complexes With Chlorocarbons.** Previously reported silylene complexes of the type  $[\text{Cp}^*(\text{Me}_3\text{P})_2\text{Ru}=\text{SiR}_2]^+$  are stable in dichloromethane solution for hours at room temperature and can be recrystallized from this solvent.<sup>7f,h</sup> It was therefore surprising to observe the rapid decomposition of nascent osmium silylene complexes upon their attempted synthesis in dichloromethane. Also, addition of dichloromethane or benzyl chloride to fluorobenzene solutions of isolated osmium silylene complexes **6** and **7** resulted in decomposition to a mixture of products similar to those observed when their synthesis was attempted in dichloromethane.

When a  $\text{CD}_2\text{Cl}_2$  solution of **5** was treated with an equivalent of  $\text{Li}[\text{B}(\text{C}_6\text{F}_5)_4] \cdot \text{Et}_2\text{O}$ , a rapid color change from yellow to brownish green was observed. Broad resonances spread over a range of 40 ppm in the  $^1\text{H}$  NMR spectrum indicated the presence of paramagnetic products in the reaction mixture. An EPR spectrum acquired at liquid helium temperature within seconds of combining a fluorobenzene solution of **6** with a stoichiometric amount of dichloromethane confirmed the presence of an Os(III) species ( $g_1 = 1.82$ ,  $g_2 = 2.29$ ,  $g_3 = 2.43$ ).<sup>27</sup> When **6** was treated with benzyl chloride, radical-termination products such as  $\text{PhCH}_2\text{CH}_2\text{Ph}$  and toluene were detected in solution by NMR spectroscopy. These data strongly indicate that the silylene complex reacts via a radical pathway involving abstraction of a chlorine atom by the silicon center to form an Os(III) species (eq 2).



To confirm its identity, a trapping experiment in which the paramagnetic Os(III) product could be con-

verted to a diamagnetic Os(II) species was undertaken. Addition of benzyl chloride to a solution of **6** immediately followed by the addition of a stoichiometric amount of the one-electron reductant  $\text{Cp}_2\text{Co}$  afforded equimolar amounts of  $\text{Cp}^*(\text{Me}_3\text{P})_2\text{OsSiMe}_2\text{Cl}$  and  $[\text{Cp}_2\text{Co}][\text{B}(\text{C}_6\text{F}_5)_4]$  as the main species in solution. Thus, the Os(III) species resulting from chlorine atom abstraction can be formulated as  $[\text{Cp}^*(\text{Me}_3\text{P})_2\text{OsSiMe}_2\text{Cl}][\text{B}(\text{C}_6\text{F}_5)_4]$ . The unusual redox process shown in Scheme 4 can therefore be proposed for the overall reaction between the osmium silylene complexes and chlorocarbons. This mechanism features chlorine atom abstraction by the Lewis acidic silylene center with concomitant formation of a carbon-centered radical. Consistent with a radical pathway and contrasting with the rapid reactivity of chlorocarbons toward **6**,  $\text{CH}_3\text{I}$  does not react with **6** within 2 days in fluorobenzene solution at room temperature. The failure of **6** to react with  $\text{CH}_3\text{I}$  reflects both the lower stability of the  $\cdot\text{CH}_3$  radical compared to the  $\cdot\text{CH}_2\text{Cl}$  and  $\text{C}_6\text{H}_5\text{CH}_2\cdot$  radicals and the greater bond strength of  $\text{Si}-\text{Cl}$  compared to that of  $\text{Si}-\text{I}$ .

In hopes of elucidating the nature of chlorine atom transfer to silicon in the reaction of **6** with chlorocarbons, a fluorobenzene solution of **6** was treated with a 1:1 mixture of benzyl chloride and 2- $\alpha$ -chloroisodurene. The less sterically demanding chlorine source, benzyl chloride, was consumed in a ratio of 30:1 as determined by NMR spectroscopy, showing that chlorine atom transfer to silicon proceeds via an intimate interaction between the two species.

From a conceptual standpoint, the reactivity promoted by the interaction between an easily oxidized, electron-rich metal center and a formally electron-deficient, Lewis acidic silylene substituent is of particular interest. The reactivity of **6** and **7** toward chlorocarbons represents a new reaction type for transition metal silylene complexes, oxidative halogen atom abstraction. This reactivity relates to the proposed intermediacy of surface-bound silylene complexes in the Rochow direct process, in which elemental silicon and chlorocarbons are converted into alkylchlorosilanes.<sup>3,28</sup> Although the mechanistic details of this industrially important, heterogeneous process are not entirely understood, silylene species such as  $:\text{SiMeCl}$  and  $:\text{SiCl}_2$

(27) Gross, C. L.; Girolami, G. S. *Organometallics* **1996**, *15*, 5359.

Table 2. Experimental Details for X-ray Crystallography

	2	3	6
empirical formula	C <sub>22</sub> H <sub>47</sub> ClP <sub>2</sub> OsSi	C <sub>23</sub> H <sub>47</sub> P <sub>2</sub> O <sub>3</sub> OsSSi	C <sub>42</sub> H <sub>39</sub> F <sub>20</sub> OsP <sub>2</sub> SiB
fw	627.3	740.9	1214.8
cryst color, habit	pale yellow block	pale pink prism	yellow block
cryst size (mm)	0.3 × 0.3 × 0.2	0.2 × 0.175 × 0.15	0.3 × 0.3 × 0.2
cryst syst	monoclinic	orthorhombic	orthorhombic
space group	<i>P</i> 2 <sub>1</sub> / <i>n</i> (#14)	<i>P</i> 2 <sub>1</sub> 2 <sub>1</sub> 2 <sub>1</sub> (#19)	<i>Pbca</i> (#61)
<i>a</i> (Å)	9.886(3)	10.1360(2)	16.7036(6)
<i>b</i> (Å)	18.5688(6)	15.176(2)	19.1576(7)
<i>c</i> (Å)	14.5933(5)	19.4838(3)	28.0680(5)
α (deg)	90	90	90
β (deg)	95.430(1)	90	90
γ (deg)	90	90	90
volume (Å <sup>3</sup> )	2666.9(5)	2997.0(3)	8981.8(5)
no. of orientation Reflns	6372	8192	8192
2θ range (deg)	3.4–52.11	3.4–52.16	3.4–52.3
<i>Z</i>	4	4	8
<i>D</i> <sub>calc</sub> (g/cm <sup>3</sup> )	1.56	1.64	1.80
<i>F</i> <sub>000</sub>	1264	1488	4768
μ(Mo Kα) (cm <sup>-1</sup> )	50.5	45.1	30.6
temperature (°C)	-152	-118	-113
data collected 2θ <sub>max</sub> (deg)	52.11	52.16	52.3
no. of reflns measd, total	12 630	14 214	35 864
no. of reflns measd, unique	4884	5310	8909
<i>R</i> <sub>int</sub>	0.056	0.047	0.079
transmn factors, <i>T</i> <sub>min</sub> / <i>T</i> <sub>max</sub>	0.37/0.53	0.31/0.41	0.36/0.65
no. of obsd data <i>I</i> > 3σ	2845	4461	3056
no. of params refined	239	307	408
refln/param ratio	12.99	14.53	7.49
final residuals <i>R</i> ; <i>R</i> <sub>w</sub> ; <i>R</i> <sub>all</sub> <sup>a</sup>	0.037; 0.041; 0.080	0.034; 0.037; 0.043	0.053; 0.055; 0.121
goodness of fit indicator <sup>b</sup>	1.05	1.41	1.68
max. shift/error in final LS cycle	0.00	0.03	0.01
max. and min. peaks (e <sup>-</sup> /Å <sup>3</sup> )	2.06/-1.89	0.67/-0.87	2.24/-1.33
	7·0.5 C <sub>6</sub> H <sub>14</sub>	8·2 C <sub>6</sub> H <sub>5</sub> F	9
empirical formula	C <sub>49</sub> H <sub>54</sub> BF <sub>20</sub> OsP <sub>2</sub> Si	C <sub>92</sub> H <sub>76</sub> B <sub>2</sub> F <sub>42</sub> N <sub>2</sub> Os <sub>2</sub> P <sub>4</sub>	C <sub>40</sub> H <sub>33</sub> BF <sub>20</sub> OsP <sub>2</sub> S
fw	1314.0	2533.5	1188.7
cryst color, habit	yellow block	yellow plate	turquoise blade
cryst size (mm)	0.35 × 0.2 × 0.2	0.24 × 0.12 × 0.15	0.15 × 0.1 × 0.05
cryst syst	triclinic	triclinic	triclinic
space group	<i>P</i> 1̄ (#2)	<i>P</i> 1̄ (#2)	<i>P</i> 1̄ (#2)
<i>a</i> (Å)	12.6468(2)	12.7080(5)	12.0406(2)
<i>b</i> (Å)	14.0345(2)	15.4596(6)	12.9290(4)
<i>c</i> (Å)	16.5265(1)	27.274(1)	15.5404(2)
α (deg)	74.799(1)	78.022(1)	111.937(2)
β (deg)	69.651(1)	78.776(1)	100.781(2)
γ (deg)	76.226(1)	66.709(1)	102.205(2)
volume (Å <sup>3</sup> )	2618.81(6)	4776.5(3)	2096.8(1)
no. of orientation reflns	8192	8092	3279
2θ range (deg)	3.4–52.3	3.4–52.2	3.4–47.95
<i>Z</i>	2	2	2
<i>D</i> <sub>calc</sub> (g/cm <sup>3</sup> )	1.67	1.73	1.88
<i>F</i> <sub>000</sub>	1310	2464	1160
μ(Mo Kα) (cm <sup>-1</sup> )	26.2	28.5	32.9
temperature (°C)	-124	-107	-112
data collected 2θ <sub>max</sub> (deg)	52.25	52.2	48.1
no. of reflns measd, total	14 605	28 312	13 033
no. of reflns measd, unique	8924	16 349	6532
<i>R</i> <sub>int</sub>	0.036	0.045	0.072
transmn factors, <i>T</i> <sub>min</sub> / <i>T</i> <sub>max</sub>	0.56/0.77	0.49/0.70	0.49/0.77
no. of obsd data <i>I</i> > 3σ	7647	8770	3685
no. of params refined	667	977	461
refln/param ratio	11.46	8.98	7.99
final residuals <i>R</i> ; <i>R</i> <sub>w</sub> ; <i>R</i> <sub>all</sub> <sup>a</sup>	0.028; 0.034; 0.035	0.037; 0.040; 0.089	0.044; 0.040; 0.09
goodness of fit indicator <sup>b</sup>	1.18	1.07	1.07
max. shift/error in final LS cycle	0.00	0.00	0.00
max. and min. peaks (e <sup>-</sup> /Å <sup>3</sup> )	2.10/-0.96	1.05/-0.64	1.92/-1.20

$$^a R = \sum ||F_o| - |F_c|| / \sum |F_o|. \quad R_w = [\sum w(|F_o| - |F_c|)^2 / \sum w F_o^2]^{1/2}. \quad ^b \text{GOF} = [\sum w(|F_o| - |F_c|)^2 / (N_{\text{obs}} - N_{\text{param}})]^{1/2}.$$

bound to copper in the Cu/Si “contact mass” are believed to react with chloromethane to afford products such as Me<sub>2</sub>SiCl<sub>2</sub> and MeSiCl<sub>3</sub>.<sup>3</sup> Although the reaction between **6** and **7** and chlorocarbons parallels only one aspect of the complex reaction pathway of the direct process, it is significant that for the first time a molecular silylene

complex has been shown to exhibit direct process-like activity by combining with chlorocarbons and forming new bonds to silicon.

**Reactions of Osmium Silylene Complexes with O and S Atom Sources.** An intriguing synthetic goal in organosilicon chemistry that has not yet been realized

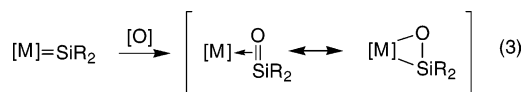
is the isolation and characterization of a silanone,  $\text{RR}'\text{Si}=\text{O}$ , either as a discrete molecular species or as a complex with a transition metal.<sup>29</sup> As the silicon analogues of ketones, silanones should possess a silicon–oxygen double bond. The study of these reactive species has been limited to matrix isolation and gas-phase experiments<sup>30</sup> and observation of their oligomerization products. For example, reactions that generate  $\text{Me}_2\text{Si}=\text{O}$  typically lead to mixtures of the cyclic oligomers  $(\text{Me}_2\text{SiO})_n$ , where  $n = 2-5$ .<sup>31</sup>

A previously employed strategy used in the synthesis of metal-free species containing  $\text{Si}=\text{S}$  (silanethione) and  $\text{Si}=\text{Se}$  (silaneselenone) groups relies on the kinetic stabilization provided by sterically demanding substituents on silicon.<sup>32</sup> This strategy has not been successfully employed in the synthesis of a free or coordinated silanone.

Computational studies have indicated that complexation in an  $\eta^2$  fashion to an appropriate transition metal fragment may stabilize a silanone against oligomerization and other decomposition pathways.<sup>33</sup> Complexes in which a silanone is bound side-on to a metal are analogous to  $\eta^2$ -transition metal ketone complexes, of which several examples are known.<sup>34</sup> The general strategy of using a transition metal to stabilize a reactive or otherwise unstable silicon species by complexation is well-precedented.

Milstein and co-workers have recently reported a catalytic system based on a bis-phosphine platinum complex that converts  $\text{HOSi}(\text{H})\text{Pr}_2$  to the cyclic trimer of diisopropylsilanone  $(\text{OSiPr}_2)_3$  and  $\text{H}_2$ .<sup>35</sup> Their proposed catalytic cycle includes a platinum-silanone species as a key intermediate, but a complex of this type could not be isolated.

Oxidation of  $:\text{SiMe}_2$  (generated by photolysis of  $(\text{Me}_2\text{Si})_6$  in an argon matrix) at low temperature by the oxygen atom transfer reagent  $\text{N}_2\text{O}$  has been shown to afford  $\text{O}=\text{SiMe}_2$ , which oligomerizes at temperatures above 80 K. It therefore seemed reasonable that a similar reaction with an isolable silylene complex such as **7** might afford a stable silanone complex (eq 3).



Treatment of **7** with soluble O atom sources such as  $\text{N}_2\text{O}$ , pyridine *N*-oxide, and 2-picoline *N*-oxide led to the

(28) (a) Rochow, E. G.; Gilliam, W. *J. Am. Chem. Soc.* **1941**, *63*, 798. (b) Seyferth, D. *Organometallics* **2001**, *20*, 4978.

(29) (a) Tokitoh, N.; Okazaki, R. *Adv. Organomet. Chem.* **2001**, *47*, 121. (b) Tokitoh, N.; Okazaki, R. In *The Chemistry of Organosilicon Compounds*, Vol. 2; Rappoport, Z., Apeloig, Y., Eds.; Wiley & Sons: New York, 1998; Chapter 17.

(30) (a) Davidson, I. M. T.; Thompson, J. F. *J. Chem. Soc., Faraday Trans. 1* **1975**, *71*, 2260. (b) Davidson, I. M. T.; Thompson, J. F. *J. Chem. Soc., Faraday Trans. 1* **1976**, *72*, 1088. (c) Davidson, I. M. T.; Fenton, A.; Manuel, G.; Bertrand, G. *Organometallics* **1985**, *4*, 1324. (d) Davidson, I. M. T.; Fenton, A. *Organometallics* **1985**, *4*, 2060.

(31) (a) Arrington, C. A.; West, R.; Michl, J. *J. Am. Chem. Soc.* **1983**, *105*, 6176. (b) Patyk, A.; Sander, W.; Gauss, J.; Cremer, D. *Angew. Chem., Int. Ed. Engl.* **1989**, *28*, 898.

(32) (a) Suzuki, H.; Tokitoh, N.; Nagase, S.; Okazaki, R. *J. Am. Chem. Soc.* **1994**, *116*, 11578–11579. (b) Suzuki, H.; Tokitoh, N.; Okazaki, R.; Nagase, S.; Goto, M. *J. Am. Chem. Soc.* **1998**, *120*, 11096. (c) Tokitoh, N.; Sadahiro, T.; Hatano, K.; Sasaki, T.; Takeda, N.; Okazaki, R. *Chem. Lett.* **2002**, 34.

(33) (a) Uzan, O.; Martin, J. M. L. *Chem. Phys. Lett.* **1998**, *290*, 535. (b) Uzan, O.; Gozin, Y.; Martin, J. M. L. *Chem. Phys. Lett.* **1998**, *288*, 356.

formation of the dinitrogen-bridged osmium dication  $[\text{Cp}^*(\text{Me}_3\text{P})_2\text{Os}-\text{NN}-\text{Os}(\text{PMe}_3)_2\text{Cp}^*][\text{B}(\text{C}_6\text{F}_5)_4]_2$  (**8**) and the cyclic siloxane trimer  $(\text{OSiPr}_2)_3$ . This cyclic siloxane, identified by NMR spectroscopy, is the same silanone trimer observed by Milstein et al. in the catalytic dehydrogenative trimerization of  $\text{HOSi}(\text{H})\text{Pr}_2$ .

In the reaction of **7** with 2-picoline *N*-oxide in fluoro-benzene solution in an NMR tube at  $-35^\circ\text{C}$ , an intermediate with two magnetically distinct  $^{31}\text{P}$  resonances was detected by NMR spectroscopy. The concentration of this intermediate did not build up appreciably, but it can be tentatively formulated as the  $\eta^2$ -diisopropylsilanone complex depicted in Scheme 5. The dissociation of this putative silanone ligand would result in formation of the coordinatively unsaturated  $\text{Cp}^*(\text{Me}_3\text{P})_2\text{Os}^+$  fragment, which could then be trapped by  $\text{N}_2$  to afford the observed dinuclear dinitrogen complex. When carried out under an atmosphere of high-purity argon, the reaction of **7** and 2-picoline *N*-oxide also led to the formation of **8** instead of an isolable silanone or picoline complex. At first quite surprising, this result can be understood in terms of the enormous avidity of  $\text{Cp}^*(\text{R}_3\text{P})_2\text{Ru}^+$  fragments for  $\text{N}_2$ .<sup>36</sup> Such fragments have been observed to efficiently scavenge  $\text{N}_2$  at the low concentrations present in ultrahigh-purity argon and helium atmospheres to afford bridged and terminal dinitrogen species. The  $\text{Cp}^*(\text{Me}_3\text{P})_2\text{Os}^+$  fragment is expected to exhibit an affinity for  $\text{N}_2$  similar to, if not greater than, similar ruthenium species.

The molecular structure of **8** is shown in Figure 5. The N–N distance of 1.137(8) Å is close to the N–N distance in free  $\text{N}_2$  of 1.094 Å. The Os–N–N–Os unit is almost linear, indicating that the bridging  $\text{N}_2$  ligand is not appreciably reduced by binding to two electron-rich Os(II) centers. The two  $\text{Cp}^*(\text{Me}_3\text{P})_2\text{Os}$  fragments are rotated about the Os–Os vector by approximately  $90^\circ$ . This orientation may indicate that the two osmium centers are engaged in  $\pi$ -back-bonding to different  $\pi^*$  orbitals on the  $\text{N}_2$  ligand.

Whereas silanones are unknown as stable molecular species, there are a few reports of isolable silanethiones.<sup>32</sup> Examples of these sulfur-containing congeners of ketones have been successfully stabilized against oligomerization through the use of sterically demanding substituents on the silicon atom. Computational results have shown that the silicon–sulfur double bond is somewhat more stable than a silicon–oxygen double bond.<sup>37</sup> Unfortunately, attempts to generate a silanethione complex of osmium by the reaction of **7** with elemental sulfur led instead to a mixture containing the disulfur-bridged dication  $[\text{Cp}^*(\text{Me}_3\text{P})_2\text{Os}-\text{S}-\text{S}-\text{Os}(\text{PMe}_3)_2\text{Cp}^*][\text{B}(\text{C}_6\text{F}_5)_4]_2$  (**9**). The fate of the silylene ligand in this reaction is not known, as discrete silicon-containing species could not be identified in the complex reaction mixture by GC/MS or NMR spectroscopy.

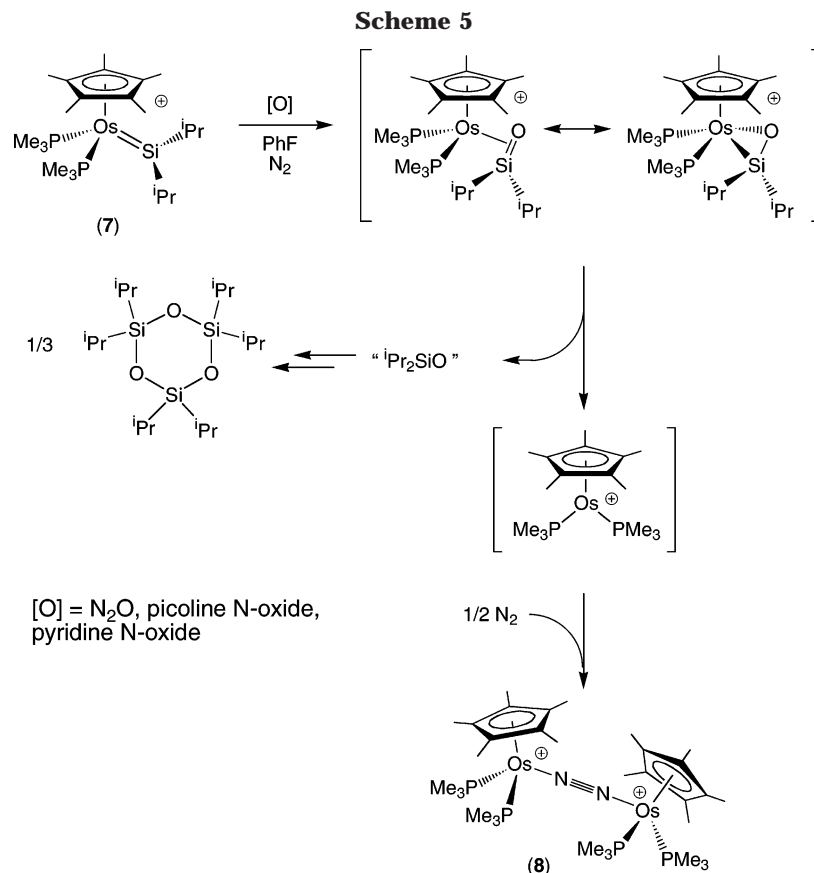
(34) (a) Gambarotta, S.; Floriani, C.; Cheisi-Villa, A.; Guastini, C. *J. Am. Chem. Soc.* **1985**, *107*, 2985. (b) Countryman, R.; Penfold, B. R. *J. Cryst. Mol. Struct.* **1972**, *2*, 281. (c) Marin, B. D.; Matchett, S. A.; Norton, J. R.; Anderson, O. P. *J. Am. Chem. Soc.* **1985**, *107*, 7952.

(35) Goikhman, R.; Aizenberg, M.; Shimon, L. J. W.; Milstein, D. *J. Am. Chem. Soc.* **1996**, *118*, 10894.

(36) Aneetha, H.; Jimenez-Tenorio, M.; Puerta, M. C.; Valerga, P.; Mereiter, K. *Organometallics* **2002**, *21*, 628.

(37) Kudo, T.; Nagase, S. *Organometallics* **1986**, *5*, 1207.





The solid state structure of **9** (Figure 6) is similar to that of the closely related ruthenium species [Cp(Me<sub>3</sub>P)<sub>2</sub>Ru–S–S–Ru(PMe<sub>3</sub>)<sub>2</sub>Cp][SbF<sub>6</sub>]<sub>2</sub>.<sup>38</sup> Both structures possess short S–S bond lengths and a metal–S–S–metal dihedral angle of 180°. Surprisingly, **9** is only sparingly soluble in fluorobenzene, but it is reasonably soluble in THF. Both in the solid state and in THF solution, **9** has a beautiful turquoise color. Similar disulfur-bridged ruthenium complexes are also strikingly colored.<sup>38</sup>

The failure of the chalcogen-atom transfer strategy to afford an isolable silanone or silanethione complex from **7** may be attributed to the lability of the target complexes and the greater stability of silanone and silanethione oligomers compared to the metal-bound

species. On the basis of the production of silanone trimerization products in the reaction between **7** and oxygen atom donors, it seems clear that the oxygen atom transfer to the silicon center to afford a transient silanone complex does, in fact, take place. With a judicious choice of metal-silylene complex, chalcogen-atom transfer may yet provide access to isolable silanone and silanethione complexes.

### Concluding Remarks

The osmium diisopropylchlorosilyl complex **2** is more conveniently prepared than the previously reported dimethylchlorosilyl complex **4**. Both of these complexes can be converted to their corresponding triflatosilyl complexes, which show significant silylene character in the solid state and in solution.

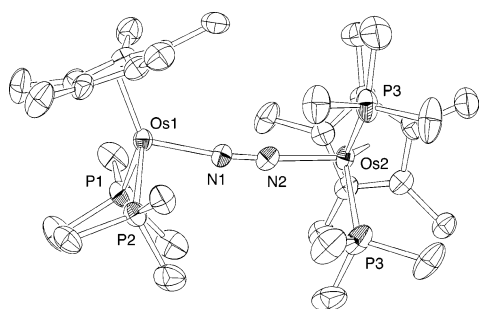


**Figure 5.** ORTEP diagram of the dinitrogen-bridged dication in **8** with thermal ellipsoids shown at the 50% probability level. Hydrogen atoms, B(C<sub>6</sub>F<sub>5</sub>)<sub>4</sub> counterions, and fluorobenzene of crystallization are omitted for clarity. The two osmium centers are crystallographically independent. Selected bond lengths (Å): Os(1)–N(1) 1.979(7), Os(2)–N(2) 1.959(8), N(1)–N(2) 1.137(8). Selected angles (deg): Os(1)–N(1)–N(2) = 172.9(7), Os(2)–N(2)–N(1) = 170.6(7).

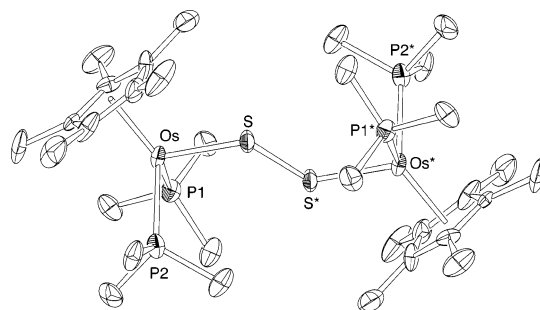


**Figure 6.** ORTEP diagram of the sulfur-bridged dication in **9** with thermal ellipsoids shown at the 50% probability level. Hydrogen atoms and B(C<sub>6</sub>F<sub>5</sub>)<sub>4</sub> counterions are omitted for clarity. A crystallographic inversion center is present between the two sulfur atoms. Selected bond lengths (Å): Os–S 2.242(3), S–S 2.017(7). Os–S–S\* angle = 125.0(3)°.

The synthesis of two base-free osmium silylene complexes **6** and **7** represents a successful extension of the anion metathesis methodology previously employed in the preparation of ruthenium silylene complexes. Similar to their ruthenium counterparts, these cationic osmium species have short bonds between an electron-rich metal center and a silicon atom in a planar, tricoordinate environment. The downfield  $^{29}\text{Si}$  chemical shifts of these complexes are also consistent with those observed for other silylene complexes.

The most intriguing difference between previously characterized metal-silylene complexes and **6** and **7** is the chlorine atom abstraction by the silicon center from chlorocarbons to afford paramagnetic Os(III) species. This reaction is apparently facilitated by the unusual combination of a Lewis acidic silylene substituent and a very electron-rich, and therefore easily oxidized, Os(II) center. This synergistic juxtaposition of two kinds of reactive centers promotes transformations not observed in previously studied systems. Formation of silicon-chlorine bonds through the reaction of silylene species with chlorocarbons may also have bearing on the mechanism of the Rochow direct process.

The attempted syntheses of osmium silanone and silanethione complexes from **7** by O or S atom transfer, respectively, was hampered by the apparent lability of the target complexes and the instability of the free silanones and silanethiones. However, as the  $\text{Cp}^*(\text{Me}_3\text{P})_2\text{Os}^+$  fragment appears to be robust enough to tolerate the chalcogen-atom transfer reaction, the method merits further investigation.

## Experimental Section

**General Procedures.** Manipulations involving air-sensitive compounds were conducted using standard Schlenk techniques under a purified  $\text{N}_2$  atmosphere or in a Braun Uni-Lab drybox. In general, solvents were distilled under  $\text{N}_2$  from appropriate drying agents and stored in PTFE-valved flasks. Deuterated solvents (Cambridge Isotopes) were dried with appropriate drying agents and vacuum-transferred before use. Reactions involving chlorosilanes or  $\text{Me}_3\text{SiOTf}$  were conducted in vessels that had been pretreated with a 9:1 mixture of  $\text{CHCl}_3/\text{Me}_3\text{SiCl}$ , air-dried, rinsed with deionized water and acetone, and oven dried.

$\text{Li}[\text{B}(\text{C}_6\text{F}_5)_4] \cdot 3\text{Et}_2\text{O}$ , **1**, **4**, and **5**<sup>18</sup> were prepared as previously described.  $^1\text{Pr}_2\text{Si}(\text{H})\text{Cl}$  was purchased from Gelest Co., purified by vacuum transfer from  $\text{CaH}_2$ , and stored in a silylated PTFE-valved storage flask.  $\text{Me}_3\text{SiOTf}$  was purchased from Aldrich, purified by vacuum transfer, and stored in a silylated PTFE-valved storage flask. Elemental sulfur, picoline *N*-oxide, and pyridine *N*-oxide were purchased from Aldrich and purified by vacuum sublimation.

$^1\text{H}$  (500.1 MHz),  $^{13}\text{C}\{^1\text{H}\}$  (124.7 MHz),  $^{31}\text{P}\{^1\text{H}\}$  (202.4 MHz), and  $^{29}\text{Si}\{^1\text{H}\}$  (99.3 MHz) NMR spectra were acquired on a Bruker DRX-500 spectrometer equipped with a 5 mm BBI probe. Spectra were recorded at room temperature and were referenced to protic impurities in the deuterated solvent for  $^1\text{H}$ , solvent peaks for  $^{13}\text{C}$ ,  $\text{SiMe}_4$  for  $^{29}\text{Si}$ , and 85%  $\text{H}_3\text{PO}_4$  for  $^{31}\text{P}$ . The HMBC experiment used to detect  $^{29}\text{Si}$  resonances has an estimated resolution of 1 ppm under typical conditions. Multiplets that appear as virtual triplets or quartets are

denoted as "vt" or "vq", respectively. The  $^{13}\text{C}$  resonances assigned to the  $\text{B}(\text{C}_6\text{F}_5)_4$  anion, or to the  $-\text{CF}_3$  group of triflate, are not reported. Combustion analyses were performed by the University of California, Berkeley College of Chemistry Microanalytical Facility.

**$\text{Cp}^*(\text{Me}_3\text{P})_2\text{OsSi}^1\text{Pr}_2\text{Cl}$  (**2**).** A PTFE-valved heavy-walled sealable reaction flask equipped with a small magnetic stirbar was charged with 217 mg (0.377 mmol) of  $\text{Cp}^*(\text{Me}_3\text{P})_2\text{OsCH}_2\text{-SiMe}_3$  and approximately 5 mL of neat  $^1\text{Pr}_2\text{Si}(\text{H})\text{Cl}$  and sealed. The reaction mixture was stirred at 100–105 °C for 36 h, and then all volatile components were removed in vacuo. The yellow residue was extracted with three 10 mL portions of warm pentane, and the combined extracts were cooled to –80 °C to afford a pale yellow, crystalline solid. Unreacted  $^1\text{Pr}_2\text{Si}(\text{H})\text{Cl}$  was recovered and repurified for use in subsequent reactions. Yield: 205 mg (85%).  $^1\text{H}$  NMR ( $\text{CD}_2\text{Cl}_2$ ,  $\delta$ ): 1.84 (s, 15 H,  $\text{C}_5\text{Me}_5$ ), 1.56 (vt,  $J = 8.4$  Hz, 18 H,  $(\text{PMe}_3)_2$ ), 1.27 (sept,  $^3J = 7$  Hz, 2 H,  $\text{Si}(\text{CHMeMe}_2)$ ), 1.05 (d,  $^3J = 7$  Hz, 6 H,  $\text{Si}(\text{CHMeMe}_2)$ ), 1.03 (d,  $^3J = 7$  Hz, 6 H,  $\text{Si}(\text{CHMeMe}_2)$ ).  $^{13}\text{C}\{^1\text{H}\}$  NMR ( $\text{CD}_2\text{Cl}_2$ ,  $\delta$ ): 90.07 ( $\text{C}_5\text{Me}_5$ ), 24.80 (m,  $\text{PMe}_3$ ), 22.64, 22.57, 19.62 ( $\text{Si}^1\text{Pr}_2$ ), 12.17 ( $\text{C}_5\text{Me}_5$ ).  $^{31}\text{P}\{^1\text{H}\}$  NMR ( $\text{CD}_2\text{Cl}_2$ ,  $\delta$ ): –51.15.  $^{29}\text{Si}$  ( $\text{CD}_2\text{Cl}_2$ , HMBC,  $\delta$ ): 61. Anal. Calcd for  $\text{C}_{22}\text{H}_{47}\text{ClO}_2\text{P}_2\text{Si}$ : C, 42.12; H, 7.55. Found: C, 42.43; H, 7.34.

**$\text{Cp}^*(\text{Me}_3\text{P})_2\text{OsSi}^1\text{Pr}_2\text{OTf}$  (**3**).** To a concentrated solution of 250 mg (0.369 mmol) of  $\text{Cp}^*(\text{Me}_3\text{P})_2\text{OsSi}^1\text{Pr}_2\text{Cl}$  in approximately 5 mL of  $\text{CH}_2\text{Cl}_2$  was slowly added a 2-fold excess of  $\text{Me}_3\text{SiOTf}$  (190 mg, 0.805 mmol) at –30 °C with constant stirring, causing a rapid color change to lemon yellow. After 1 h of stirring at ambient temperature, the volume of the reaction mixture was reduced in vacuo to a volume of approximately 2 mL, and the solution was layered with diethyl ether. Cooling to –30 °C afforded large, well-formed hexagonal crystals suitable for X-ray analysis. Yield: 215 mg (72.8%).  $^1\text{H}$  NMR ( $\text{CD}_2\text{Cl}_2$ ,  $\delta$ ): 1.90 (t,  $J = 1$  Hz, 15 H,  $\text{C}_5\text{Me}_5$ ), 1.84 (sept,  $^3J = 7.5$  Hz, 2 H,  $\text{Si}(\text{CHMe}_2)_2$ ), 1.65 (vt,  $J = 8.5$  Hz, 18 H,  $(\text{PMe}_3)_2$ ), 1.18 (d,  $^3J_{\text{HH}} = 7.5$  Hz, 12 H  $\text{Si}(\text{CHMe}_2)_2$ ).  $^{13}\text{C}\{^1\text{H}\}$  NMR ( $\text{CD}_2\text{Cl}_2$ ,  $\delta$ ): 92.72 ( $\text{C}_5\text{Me}_5$ ), 30.98 ( $\text{Si}(\text{CHMe}_2)_2$ ), 26.67 (m,  $(\text{PMe}_3)_2$ ), 18.85 ( $\text{Si}(\text{CHMe}_2)_2$ ), 11.84 ( $\text{C}_5\text{Me}_5$ ).  $^{29}\text{Si}$  (HMBC,  $\text{C}_6\text{D}_6$ ,  $\delta$ ): 100.  $^{29}\text{Si}$  (HMBC,  $\text{CD}_2\text{Cl}_2$ ,  $\delta$ ): 223.  $^{31}\text{P}\{^1\text{H}\}$  NMR ( $\text{CD}_2\text{Cl}_2$ ,  $\delta$ ): –48.8. Anal. Calcd for  $\text{C}_{23}\text{H}_{47}\text{P}_2\text{O}_3\text{OSi}$ : C, 37.28; H, 6.39. Found: C, 37.07; H, 6.44.

**$[\text{Cp}^*(\text{Me}_3\text{P})_2\text{Os}=\text{SiMe}_2][\text{B}(\text{C}_6\text{F}_5)_4]$  (**6**).** To a –35 °C solution of **5** (100 mg, 0.146 mmol) in fluorobenzene (2 mL) was added 1.1 equiv of  $\text{Li}[\text{BC}_6\text{F}_5]_4 \cdot \text{Et}_2\text{O}$  (140 mg, 0.163 mmol) as a fluorobenzene solution at –35 °C. A color change to bright lemon yellow and the formation of a white precipitate were immediately observed. The reaction mixture was filtered to remove insoluble materials. Solvents were removed in vacuo, and the resulting solid was titrated with hexanes (3 × 3 mL) to afford a bright yellow solid. Yield: 85 mg (48%).  $^1\text{H}$  NMR ( $\text{C}_6\text{H}_5\text{F}$ ,  $\text{C}_6\text{D}_6$  external standard,  $\delta$ ): 1.57 (s, 15 H,  $\text{C}_5\text{Me}_5$ ), 1.25 (vt,  $J = 8.8$  Hz, 18 H,  $(\text{PMe}_3)_2$ ), 0.65 (s, 6 H,  $\text{SiMe}_2$ ).  $^{13}\text{C}\{^1\text{H}\}$  NMR ( $\text{C}_6\text{H}_5\text{F}$ ,  $\text{C}_6\text{D}_6$  external standard,  $\delta$ ): 94.32 ( $\text{C}_5\text{Me}_5$ ), 24.53 (vt,  $J = 53.4$  Hz,  $(\text{PMe}_3)_2$ ), 15.12 ( $\text{SiMe}_2$ ), 10.43 (s,  $\text{C}_5\text{Me}_5$ ).  $^{29}\text{Si}$  NMR (HMBC,  $\text{C}_6\text{H}_5\text{F}$ ,  $\text{C}_6\text{D}_6$  external standard,  $\delta$ ): 350.  $^{31}\text{P}\{^1\text{H}\}$  NMR ( $\text{C}_6\text{H}_5\text{F}$ ,  $\delta$ ): –49.9. Anal. Calcd for  $\text{C}_{42}\text{H}_{39}\text{BF}_{20}\text{OsP}_2\text{-Si}$ : C, 41.53; H, 3.24. Found: C, 41.34; H, 3.43.

**$[\text{Cp}^*(\text{Me}_3\text{P})_2\text{Os}=\text{Si}^1\text{Pr}_2][\text{B}(\text{C}_6\text{F}_5)_4]$  (**7**).** Compound **3** (85 mg, 0.11 mmol) was dissolved in approximately 5 mL of fluorobenzene, and the resulting solution was treated at –10 °C with a fluorobenzene solution of 96 mg (0.12 mmol) of freshly prepared  $\text{Li}[\text{BC}_6\text{F}_5]_4 \cdot 3\text{Et}_2\text{O}$ , with stirring. The reaction mixture became turbid after 5 min and was allowed to settle. The resulting suspension was filtered through a PTFE syringe filter to remove  $\text{LiOTf}$  and was then layered with hexanes. After 10 days at –30 °C, large, blocky crystals were obtained. These crystals were rinsed with hexane and dried in vacuo to afford a yellow powder. Yield: 73 mg (51%).  $^1\text{H}$  NMR ( $\text{C}_6\text{H}_5\text{F}$ ,  $\text{C}_6\text{D}_6$  external standard,  $\delta$ ): 2.20 (sept,  $^3J = 7.5$  Hz, 2 H,  $\text{Si}(\text{CHMe}_2)_2$ ), 1.81 (s, 15 H,  $\text{C}_5\text{Me}_5$ ), 1.56 (vt,  $J = 8$  Hz, 18 H,  $(\text{PMe}_3)_2$ ), 1.19 (d,  $^3J = 8$  Hz, 12 H,  $\text{Si}(\text{CHMe}_2)_2$ ).  $^{13}\text{C}\{^1\text{H}\}$  NMR

(38) Amarasekera, J.; Rauchfuss, T. B.; Wilson, S. R. *Inorg. Chem.* **1987**, *26*, 3328.

(39) Massey, A. G.; Park, A. J. *J. Organomet. Chem.* **1964**, *2*, 245. The amount of  $\text{Et}_2\text{O}$  present in the material prepared by the route published here varied from 1 to 3 equiv and was determined by combustion analysis.

(C<sub>6</sub>H<sub>5</sub>F, C<sub>6</sub>D<sub>6</sub> external standard,  $\delta$ ): 93.35 (C<sub>5</sub>Me<sub>5</sub>), 36.11 (Si(CHMe<sub>2</sub>)<sub>2</sub>), 24.52 (m, (PMe<sub>3</sub>)<sub>2</sub>), 15.75 ((Si(CHMe<sub>2</sub>)<sub>2</sub>), 10.20 (C<sub>5</sub>Me<sub>5</sub>). <sup>29</sup>Si (HMBC, C<sub>6</sub>H<sub>5</sub>F, C<sub>6</sub>D<sub>6</sub> external standard,  $\delta$ ): 365. <sup>31</sup>P{<sup>1</sup>H} NMR (C<sub>6</sub>H<sub>5</sub>F,  $\delta$ ): 51.90. Anal. Calcd for C<sub>46</sub>H<sub>17</sub>BF<sub>20</sub>-OsP<sub>2</sub>Si: C, 43.47; H, 3.73. Found: C, 43.58; H, 4.06

**[Cp\*(Me<sub>3</sub>P)<sub>2</sub>Os-NN-Os(PMe<sub>3</sub>)<sub>2</sub>Cp\*][B(C<sub>6</sub>F<sub>5</sub>)<sub>4</sub>]<sub>2</sub> (8).** A degassed fluorobenzene solution (10 mL) of **7** (191 mg, 0.150 mmol) was degassed and exposed to an atmosphere of N<sub>2</sub>O. The solution was agitated vigorously, causing a color change from intense lemon yellow to pale yellow. The reaction mixture was concentrated in vacuo to approximately 5 mL and layered with 5 mL of pentane. After 2 days at -10 °C, a microcrystalline precipitate had formed. The product was isolated by filtration and washed with two 5 mL portions of pentane and dried in vacuo. Yield: 129 mg (73%). <sup>1</sup>H NMR (C<sub>6</sub>H<sub>5</sub>F + 10% C<sub>6</sub>D<sub>6</sub>,  $\delta$ ): 1.31 (t, *J*<sub>PH</sub> = 1.2 Hz, 15 H, C<sub>5</sub>Me<sub>5</sub>), 1.00 (vt, *J* = 8.5 Hz, (PMe<sub>3</sub>)<sub>2</sub>). <sup>13</sup>C{<sup>1</sup>H} NMR (90% C<sub>6</sub>H<sub>5</sub>F + 10% C<sub>6</sub>D<sub>6</sub>,  $\delta$ ): 92.39 (t, *J*<sub>CP</sub> = 1.8 Hz, C<sub>5</sub>Me<sub>5</sub>), 18.52 (m, (PMe<sub>3</sub>)<sub>2</sub>), 9.47 (C<sub>5</sub>Me<sub>5</sub>). <sup>31</sup>P{<sup>1</sup>H} NMR (CD<sub>2</sub>Cl<sub>2</sub>,  $\delta$ ): 50.19. Anal. Calcd for C<sub>80</sub>H<sub>66</sub>B<sub>2</sub>F<sub>40</sub>P<sub>4</sub>N<sub>2</sub>-Os<sub>2</sub>: C, 41.04; H, 2.84. Found: C, 41.23; H, 3.09.

**[Cp\*(Me<sub>3</sub>P)<sub>2</sub>Os-S-S-Os(PMe<sub>3</sub>)<sub>2</sub>Cp\*][B(C<sub>6</sub>F<sub>5</sub>)<sub>4</sub>]<sub>2</sub> (9).** A dilute fluorobenzene solution of **7** (45 mg, 0.35 mmol) in 20 mL of fluorobenzene was added to a solution of S<sub>8</sub> (1.1 mg, 0.034 mmol) in 5 mL of fluorobenzene. The resulting mixture was stirred for approximately 10 min at room temperature. Stirring was halted, and the solution turned green, then blue as it became turbid and solid **9** precipitated. Analytically pure solid was obtained by recrystallization from a THF/pentane mixture. Yield: 18 mg (43%). <sup>1</sup>H NMR (THF-*d*<sub>8</sub>,  $\delta$ ): 1.95 (s, 15 H, C<sub>5</sub>Me<sub>5</sub>), 1.59 (vt, *J* = 8 Hz, 18 H, (PMe<sub>3</sub>)<sub>2</sub>). <sup>13</sup>C{<sup>1</sup>H} NMR (THF-*d*<sub>8</sub>,  $\delta$ ): 100.91 (C<sub>5</sub>Me<sub>5</sub>), 21.63 (vt, (PMe<sub>3</sub>)<sub>2</sub>), 10.64 (C<sub>5</sub>Me<sub>5</sub>). <sup>31</sup>P{<sup>1</sup>H} NMR (THF-*d*<sub>8</sub>,  $\delta$ ): -53.85. Anal. Calcd for C<sub>40</sub>H<sub>33</sub>-BF<sub>20</sub>P<sub>2</sub>SO<sub>2</sub>: C, 40.42; H, 2.80; S, 2.70. Found: C, 40.47; H, 2.52; S, 2.50.

**X-ray Crystallography.** Crystallographic analyses were carried out at the University of California, Berkeley CHEXRAY crystallographic facility.<sup>40</sup> All measurements were made on a Bruker SMART CCD area detector with graphite-monochromated Mo K $\alpha$  radiation ( $\lambda$  = 0.71069 Å). Crystals were mounted on capillaries with Paratone-N hydrocarbon oil and held in a low-temperature N<sub>2</sub> stream during data collection. Frames were collected using  $\omega$  scans at 0.3° increments, using exposures of 10 s. Data were integrated with the program SAINT,<sup>41</sup> corrected for Lorentz and polarization effects, and analyzed for agreement and possible absorption using XPREP.<sup>42</sup> Empirical absorption corrections were made with either SADABS<sup>43</sup> or XPREP. Structures were solved by direct methods and expanded using Fourier techniques.<sup>44</sup> The quantity minimized by the least-squares program was  $\sum w(|F_o| - |F_c|)$ , where *w* is the weight of a given observation. The analytical forms of the scattering factor tables for the neutral atoms were used, and all scattering factors were corrected for both the real and the imaginary components of anomalous dispersion. Calculations were performed using the teXsan crystallographic software package.<sup>45</sup> Selected crystal and structure refinement data are summarized in the tables. In each case, the calculated

centroid of the Cp\* ring was placed in a fixed position as a carbon atom with a partial occupancy of 0.0001 and a fixed *B*<sub>iso</sub> of 0.2 and included in the final cycles of least-squares refinement. Unless stated otherwise, non-hydrogen atoms were allowed to refine anisotropically. Hydrogen atoms were placed at calculated positions and not refined.

**For 2.** Crystals of **2** were grown by slow cooling of a concentrated pentane solution to -35 °C. When all atoms were allowed to refine with anisotropic thermal parameters, one of the inner Cp\* carbon atoms, C(4), refined with a single nonpositive thermal parameter. The structure could be successfully refined to an acceptable *R* value with either C(4) or all inner Cp\* carbons set to refine isotropically. The final stages of refinement used a model in which all five inner carbons were set to refine isotropically. These difficulties are reasonably attributed to a large amount of librational motion in the Cp\* ligand. This conclusion is supported by the disposition of the prolate thermal ellipsoids of the Cp\* methyl carbon atoms. The largest residual peaks in the Fourier map are located around osmium.

**For 3.** Crystals of **3** were grown by cooling of a concentrated CH<sub>2</sub>Cl<sub>2</sub> solution layered with Et<sub>2</sub>O. The correct choice of enantiomorph of the molecule was confirmed by refinement to an acceptable *R* value and a successful Bijouvet analysis. The largest residual peaks in the Fourier map are located close to osmium.

**For 6.** Crystals were grown by vapor diffusion of pentane into a concentrated fluorobenzene solution. The Cp\* ring in this molecule is badly disordered. Of the many structural models tested, the most successful includes two partial occupancy (0.7 and 0.3) Cp\* rings treated as isotropic rigid groups. The 24 carbon atoms in the B(C<sub>6</sub>F<sub>5</sub>)<sub>4</sub> anion were allowed to refine isotropically. Although the disorder in this structure appears to be rotational disorder, the axis of rotational disorder does not coincide with an Os-Cp\*(centroid) vector. In addition, the methyl groups of the silylene ligand refine with large prolate thermal ellipsoids with major axes roughly orthogonal to the Os-Si vector. This may indicate a substantial amount of librational motion in this ligand in the solid state. The model was refined to a final *R* of 5.3. The largest residual peaks in the Fourier map are located close to osmium.

**For 7.** The structure is of especially high quality, and no difficulties were encountered in the solution or refinement. A molecule of *n*-hexane lies on the crystallographic inversion center and is well-resolved and fully ordered. The largest residual peaks in the Fourier map are located around osmium.

**For 8.** Crystals were grown from a fluorobenzene solution layered with Et<sub>2</sub>O and cooled to -30 °C. The asymmetric unit in the structure contains the entire organometallic dication, two independent B(C<sub>6</sub>F<sub>5</sub>)<sub>4</sub> anions, and two fluorobenzene molecules. In order to preserve a high data/parameter ratio, the 48 carbon atoms in the B(C<sub>6</sub>F<sub>5</sub>)<sub>4</sub> anions and all 14 atoms in the fluorobenzene molecules were allowed to refine isotropically. Other than the improved data/parameter ratio, the differences between this refinement and one in which all nonhydrogen atoms were allowed to refine anisotropically were negligible. The largest residual peaks in the Fourier map are located near one fluorobenzene ring and the osmium center.

**For 9.** Crystals were grown by slow diffusion of pentane into a THF solution. The asymmetric unit in the structure contains one-half of the organometallic dication and an B(C<sub>6</sub>F<sub>5</sub>)<sub>4</sub> anion. The inversion center in the structure lies between the two sulfur atoms of the bridged dication. To preserve a high data/parameter ratio, the 24 carbon atoms of the B(C<sub>6</sub>F<sub>5</sub>)<sub>4</sub> anion were allowed to refine isotropically. Other than the improved data/parameter ratio, the differences between this refinement and one where all nonhydrogen atoms were allowed to refine anisotropically were negligible. The largest residual peaks in the Fourier map are located near osmium.

(40) <http://xray.cchem.berkeley.edu>.

(41) SAINT: SAX Area-Detector Integration Program, version 4.024; Bruker, Inc.: Madison, WI, 1995.

(42) XPREP v. 5.03: Part of the SHELXTL Crystal Structure Determination Package; Siemens Industrial Automation, Inc.: Madison, WI, 1995.

(43) Sheldrick, G. M. SADABS: Siemens Area Detector ABSorption correction program; 1996. Advance copy, private communication.

(44) (a) Altomare, A.; Burla, M. C.; Camalli, M.; Cascarano, M.; Giacovazzo, C.; Guagliardi, A.; Polidori, G. *SIR92. J. Appl. Crystallogr.* **1992**, *26*, 343. (b) Beurskens, P. T.; Admiraal, G.; Beurskens, G.; Bosman, W. P.; Garcia-Granda, S.; Gould, R. O.; Smits, J. M. M.; Smykalla, C. *DIRDIF92: The DIRDIF Program System*; Technical Report of the Crystallography Laboratory; University of Nijmegen: The Netherlands, 1992.

(45) teXsan: Crystal Structure Analysis Package; Molecular Structure Corporation, 1985 and 1992.

**Acknowledgment.** This work was generously supported by the National Science Foundation. CNDOS is supported by Bristol-Meyers Squibb as a Sponsoring Member and Novartis Pharama as a Supporting Member. The authors wish to thank Dr. Wayne Leukens of the Lawrence Berkeley National Laboratory for obtaining EPR data, Drs. Dana Caulder, Alan Oliver, and Fred Hollander of the UC Berkeley CHEXRAY facility for assistance with X-ray crystallography, Dr. Urs Burck-

hardt for implementing the  $^{29}\text{Si}$  HMBC NMR experiment, and Professors Robert Bergman and Richard Andersen for valuable discussions.

**Supporting Information Available:** Tables of atomic coordinates, thermal displacement parameters, and selected bond lengths and angles for **2**, **3**, **6**, **7**, **8**, and **9**. This material is available free of charge via the Internet at <http://pubs.acs.org>.

OM0341808